JOURNAL OF SOLID STATE CHEMISTRY **92**, 202–207 (1991)

Structural, Magnetic, and Optical Investigation of Ni_6MnO_8

P. PORTA* AND G. MINELLI

Centro C.N.R. su "Struttura e Attività Catalitica di Sistemi di Ossidi," Dipartimento di Chimica, Università di Roma La Sapienza, Piazzale A.Moro 5, 00185 Roma, Italy

AND I. L. BOTTO AND E. J. BARAN

Departamento de Quimica, Facultad de Ciencias Exactas, Universidad Nacional de La Plata, Calles 47 y 115, 1900-La Plata, Argentina

Received July 9, 1990

Mg_6MnO_8 and Ni_6MnO_8, which contain octahedrally coordinated Mg^{2+}, Ni^{2+}, Mn^{4+}, and cation vacancies in a cubic lattice with space group *Fm3m* have been prepared. Ni_6MnO_8 has been characterized by means of several techniques. The X-ray powder pattern has shown that Ni_6MnO_8 is isomorphous to Mg_6MnO_8. The unit cell parameter, a, of Ni_6MnO_8 is 8.306 ± 0.003 Å, which, as compared with that previously found for Mg_6MnO_8 (a = 8.381 Å), agrees with expectations based on the difference between the ionic radii for Ni^{2+} and Mg^{2+} in octahedral coordination. The magnetic susceptibility measurements for Ni_6MnO_8 give the following values: C = 1.35, μ = 3.28 BM, θ = −65 K, which confirm that Ni and Mn are in oxidation states of 2+ and 4+, respectively, and that some antiferromagnetic interactions are present within the lattice among Ni^{2+} and Mn^{4+}. The reflectance spectrum performed on Ni_6MnO_8 has shown the presence of several bands which have been assigned to the d–d transitions expected for both Ni^{2+} and Mn^{4+} ions in octahedral coordination. The six bands in the IR spectra of Mg_6MnO_8 and Ni_6MnO_8 compounds have been assigned; the shift toward higher frequencies observed for Mg_6MnO_8 is in agreement with expectations since Mg^{2+} has a larger ionic radius than Ni^{2+}, and this makes the nearest Mn^{4+}–O bond shorter and stronger in the magnesium compound.

Introduction

In the last few years a great number of metallic oxides have been considered as possible oxygen sensors. So, there is an increasing interest for these compounds, which could show a better chemical and ceramic stability than the usually employed ZrO_2 sensors. Toward this goal, the M–Mn–O systems (M = Ni, Mg) have been recently analyzed (*1–3*).

Of the several nickel and manganese mixed oxides, included in the Ni–Mn–O system, little is known about the Ni_6MnO_8 phase. This compound is related to the murdochite series (Cu_6PbO_8 and Mg_6MnO_8), but unlike these compounds (*4–9*) there is not much information available about it.

The crystal structure of the $M_6M'O_8$ compounds, which are cubic with space group *Fm3m*, may be considered as derived from the MO (M = divalent cation) rock-salt structure where six-eighths of the octahedral sites are occupied by the divalent M

* To whom correspondence should be addressed.

0022-4596/91 $3.00

cation, and one-eighth each by tetravalent, M', cations and by vacancies, the latter ordered in the alternate (111) layers. Both M and M' cations are octahedrally coordinated by six oxygens. The octahedron around the tetravalent M' ions is generally regular whereas that around the divalent M ones is distorted.

This paper reports the results of a structural, magnetic, and optical investigation performed on the Ni_6MnO_8 compound. The related magnesium–manganese oxide phase has been analyzed for comparative purposes.

Experimental

Preparation. Pure samples of Ni_6MnO_8 and Mg_6MnO_8 were obtained from the respective Ni(II), Mg(II), and Mn(II) acetates by the "precursors" technique (*10, 11*). For the nickel compound the Ni(II) and Mn(II) acetates were dissolved in acetic acid (25%). The mixture of both solutions in stoichiometric ratios was boiled and vigorously stirred. A solution of oxalic acid containing the equivalent quantity of acid, plus an excess of 10%, was quickly added. The mixture was then carried to dryness at 378 K. The powder was finally pelletized and calcined in air at 873 K for 3 hr. The purity of the bright yellow–brown sample was checked by XRD, revealing the presence of the pure desired phase. Also the chemical analysis, performed by atomic absorption with a Varian SpectrAA-30 instrument, confirmed the formula Ni_6MnO_8. The other isostructural magnesium compound, used as reference, was obtained according to the method reported in the literature (*5*).

IR Spectra. The IR spectra were recorded with a Perkin–Elmer 580-B spectrophotometer using the KBr pellet technique.

Magnetic susceptibility. Magnetic susceptibilities were measured by the Gouy method over the range of temperature 100–300 K. Correction was made for the diamagnetism of the sample. A check that the susceptibilities were independent of magnetic field strength was made.

X-ray diffraction. The powder diffraction pattern was obtained with a Philips automated PW 1729 diffractometer. Scans were taken with a step size of 0.01°, using Cu$K\alpha$ (nickel-filtered) radiation. The intensities of the reflections were estimated by evaluation of the integrated peaks. The unit cell parameter for the cubic lattice of Ni_6MnO_8 was determined taking into account all reflections occurring up to $2\theta = 170°$ and applying a least-squares fit procedure on the observed 2θ values of the individual reflections.

Reflectance spectra. The diffuse reflectance spectrum was carried out by using a Cary 2300 spectrometer equipped with a diffuse reflectance accessory, in the wavelengths range from 200 to 2500 nm, covering the UV, visible, and near-infrared regions.

Results and Discussion

As shown in Table I the X-ray powder pattern of Ni_6MnO_8 is similar to that reported in the literature for the parent compound Mg_6MnO_8 (*5, 6, 12*). The lattice parameter, a, for the cubic unit cell of Ni_6MnO_8 is 8.306 ± 0.003 Å, with a volume, V, equal to 573.03 ± 0.01 Å^3. By comparing the above results with those found for Mg_6MnO_8, $a = 8.381$ Å and $V = 588.69$ Å^3 (*12*), it may be noticed that the volume shrinkage by going from the magnesium compound to the nickel containing one is in agreement with expectations based on the difference of octahedral ionic radii for Ni^{2+} and Mg^{2+} (equal to 0.69 and 0.72 Å, respectively) (*13*).

From the linear behavior observed at higher temperatures (168–294 K) in the $1/\chi_m$ vs T (Table II) plot of the magnetic measurement the following values have been determined: Curie constant, $C = 1.35$; magnetic moment, $\mu = 3.28$ BM; Weiss

TABLE I

X-RAY PATTERN OF Ni_6MnO_8: MILLER INDEXES, INTENSITIES, OBSERVED, d_o, AND CALCULATED, d_c, SPACINGS

	Ni_6MnO_8			Mg_6MnO_8	
hkl	*I*	d_o	d_c	d_o	*I*
111	25	4.800	4.809	4.84	60
200	14	4.162	4.161		
220	13	2.940	2.939		
311	13	2.506	2.505	2.53	15
222	65	2.399	2.399	2.42	11
400	100	2.077	2.077	2.10	100
331	2	1.906	1.906	1.923	5
420	10	1.858	1.858		
422	9	1.696	1.696		
333–511	10	1.599	1.599	1.613	9
440	45	1.468	1.468	1.482	50
531	9	1.404	1.404	1.417	9
600–442	5	1.385	1.384		
620	2	1.313	1.313		
533	25	1.267	1.267	1.278	1
622	2	1.253	1.252	1.263	9
444	20	1.199	1.199	1.210	16
711–551	2	1.163	1.163	1.174	5
640	2	1.152	1.152		
642	2	1.110	1.110		
731–553	2	1.082	1.081	1.091	3
800	13	1.038	1.038	1.048	7
733	1	1.014	1.015		
644–820	2	1.007	1.007		
660–822	1	0.9796	0.9789		
751–555	14	0.9596	0.9591	0.9677	3
662	1	0.9535	0.9528	0.9614	5
840	25	0.9291	0.9287	0.9370	20
911–753	2	0.9122	0.9117	0.9199	3
842	1	0.9065	0.9063		
664	1	0.8861	0.8854		
931	2	0.8703	0.8707	0.8786	3
844	20	0.8478	0.8477	0.8554	20
933–771–755	2	0.8351	0.8348	0.8423	3
860–1000	1	0.8305	0.8306		
862–1020	2	0.8144	0.8145		
951–773	1	0.8027	0.8030	0.8102	7
666–1022	1	0.7992	0.7992	0.8065	9
953	1	0.7746	0.7745	0.7815	9

Note. The X-ray pattern of the reference Mg_6MnO_8 compound is also reported (ASTM 11-31).

temperature, $\theta = -65$ K. By taking into account the values of the Curie constants expected for Ni^{2+} in octahedral coordination ($C = 1.28$ for Ni^{2+}/MgO, Ref. (*14*)) and for Mn^{4+} in Mg_6MnO_8 ($C = 1.94$, Ref. (5)], and considering the relative molar fractions, X, of Ni (0.857) and Mn (0.143) present in our sample the averaged value of the Curie constant, C, may be evaluated from the additivity law:

$$C = C_{Ni} \cdot X_{Ni} + C_{Mn} \cdot X_{Mn}$$

The calculated value of 1.37 is in agreement with the observed value of 1.35; this confirms the presence of Ni^{2+} and Mn^{4+} species in Ni_6MnO_8. It may be added that the value of -65 K found for the Weiss temperature implies that some antiferromagnetic interactions occur within the solid among the Ni^{2+} and Mn^{4+} paramagnetic ions.

The reflectance spectrum of Ni_6MnO_8, reported in Fig. 1, shows the appearance of five bands in the region 1400–350 nm (7150–28,600 cm^{-1}). By analogy to the spectra reported in the literature for Ni^{2+} (*14–17*)

TABLE II

MOLAR MAGNETIC SUSCEPTIBILITY X_m (erg · G^{-2} · $mole^{-1}$) AS MEASURED AT DIFFERENT TEMPERATURES (K) FOR Ni_6MnO_8

X_m ($\times 10^3$)	*T*
7.25	107
7.22	113
7.20	118
7.08	124
6.87	131
6.70	137
6.43	144
6.18	149
5.54	160
5.28	165
5.14	168
5.08	171
4.95	177
4.79	190
4.69	196
4.54	207
3.70	294

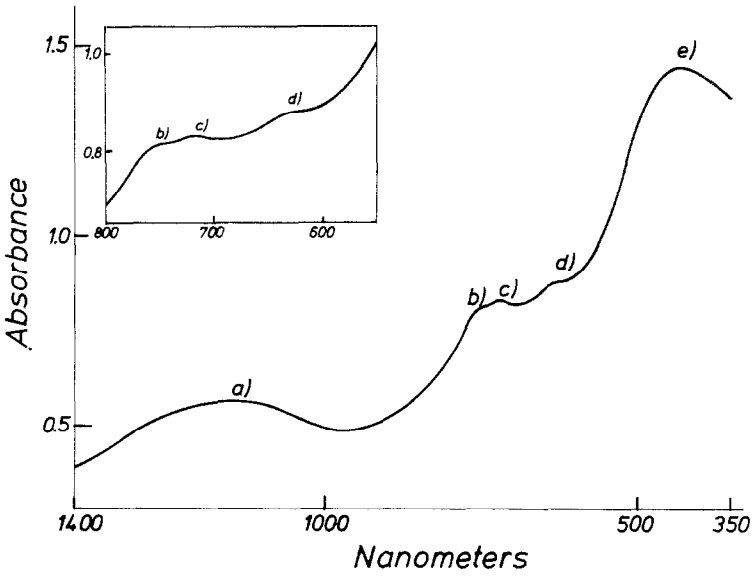

FIG. 1. Reflectance spectrum of Ni_6MnO_8. The insert shows, in an enlarged scale, the three bands occurring in the range from 600 to 800 nm.

and Mn^{4+} (*5*) in octahedral coordination the following assignments have been made:

(i) the large band (a) centered at 1150 nm (8700 cm^{-1}) is attributed to the $^3A_{2g} \rightarrow {}^3T_{2g}$ *d–d* Ni^{2+} transition;

(ii) the small bands (b), (c), and (d) (shown in an enlarged scale in the insert of Fig. 1) at 750 nm (13,300 cm^{-1}), at 718 nm (13,900 cm^{-1}), and at 630 nm (15,900 cm^{-1}), respectively, are assigned to the spin forbidden $^4A_{2g} \rightarrow {}^2E_g$, $^4A_{2g} \rightarrow {}^2T_{1g}$, and $^4A_{2g} \rightarrow {}^2T_{2g}$ Mn^{4+} transitions;

(iii) the strong band (e) centered at 430 nm (23,200 cm^{-1}) is due to the superposition of three bands, one coming from the $^3A_{2g} \rightarrow {}^3T_{1g}$, Ni^{2+} transition (it occurs at 370 nm, 27,000 cm, in $Ni^{2+}/MgAl_2O_4$, (*17*)), and two from the $^4A_{2g} \rightarrow {}^4T_{2g}$ and $^4A_{2g} \rightarrow {}^4T_{1g}$ Mn^{4+} transitions (they occur at 490 nm, 20,400 cm^{-1}, and at 410 nm, 24,400 cm^{-1}, in Mg_6MnO_8 (*5*)).

We may finally report and discuss the results obtained from the IR spectra. It should be recalled that, according to the crystal structure of the $M_6M'O_8$ parent compounds, both the bi- and tetravalent cations are octahedrally coordinated by six oxygens, although the environment around the M^{2+} cation is slightly distorted. The number and symmetry of the vibrational modes in the M_6MnO_8 spectra can be obtained by a factor group analysis (*18, 19*). Table III gives the correlation for the M_6MnO_8 compounds, which is obtained considering the atomic positions for the $Fm3m$ space group. The irreducible representation of the optical modes in the crystal lattice is:

$$\Gamma_{opt} = 6F_{1u} + A_{1g} + E_g + F_{1g} + 2F_{2g} + A_{2u} + E_u + 3F_{2u},$$

where only the F_{1u} modes are IR active. The A_{1g}, E_g, and F_{2g} vibrations are active in the Raman effect, whereas the remaining modes are inactive.

According to these results six bands must be observed in the IR spectrum and only four in the Raman effect. The latter spectrum is very difficult to obtain in our case mainly because of the darkness of the samples.

TABLE III

FACTOR GROUP ANALYSIS OF THE M_6MnO_8 LATTICE (SPACE GROUP $Fm3m$)

Atom	Number and position	A_{1g}	A_{2g}	E_g	F_{1g}	F_{2g}	A_{1u}	A_{2u}	E_u	F_{1u}	F_{2u}
Mn	1*a*	0	0	0	0	0	0	0	0	1	0
M	6*d*	0	0	0	0	0	0	1	1	3	2
O_I	2*c*	0	0	0	0	1	0	0	0	1	0
O_{II}	6*e*	1	0	1	1	1	0	0	0	2	1
Total ($3N = 45$)		1	0	1	1	2	0	1	1	7	3
Acoustic (3)										1	

Figure 2 shows the IR spectra of both Mg_6MnO_8 and Ni_6MnO_8 compounds. As it is possible to observe, the six predicted bands (whose frequencies in cm^{-1} are reported for both compounds) appear in the IR spectra.

Although the M^{2+}–Mn^{4+} atomic distances are approximately 3 Å, the existence of important coupling effects between both MO_6 polyhedra in the lattice is evident. So, all the atoms can contribute to each vibration. A similar behavior has been observed in some other oxidic systems such as the $Te_3M^{4+}O_8$ compounds (*20, 21*). However, the highest frequency bands (although not pure vibrations) might be associated with the Mn^{4+} polyhedra (*22*). By comparing the IR spectra of the two compounds a slight shift toward higher frequencies is observed for the Mg sample. This is in agreement with the M^{2+} ionic radii (0.69 and 0.72 Å for Ni^{2+} and Mg^{2+}, respectively (*13*)) whose effect is to shorten and reinforce the Mn–O bond in the magnesium compound.

The strong band located between 400 and 450 cm^{-1} may be assigned to the M^{2+}–O–Mn^{4+} stretching–shrinking motions which appear at higher frequencies than those observed in other related oxidic systems (*23*). The bands below 400 cm^{-1} are associated with the $M^{2+}O_6$ and $Mn^{4+}O_6$ bendings.

It is also interesting to remark that IR spectroscopy allows one to follow the Ni_6MnO_8 thermal behavior. We have ob-

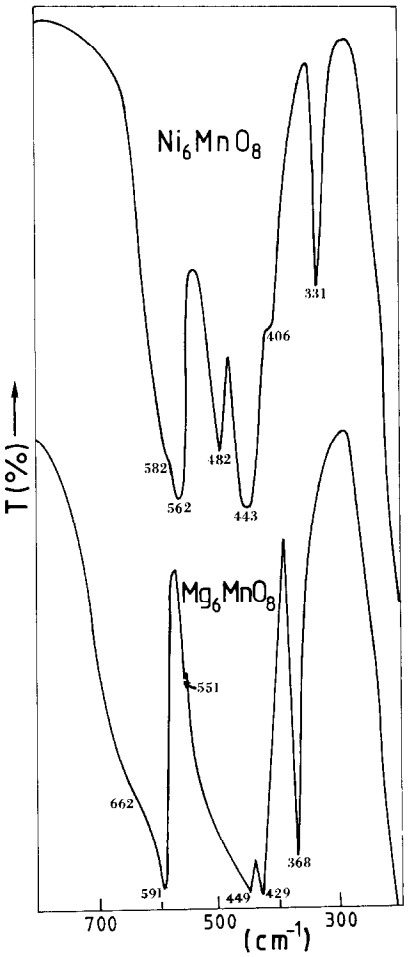

FIG. 2. IR spectra: (a) Mg_6MnO_8; (b) Ni_6MnO_8. Frequencies, cm^{-1}, are reported for each band.

served that the decomposition process starts at 1073 K with a clear segregation of NiO and $NiMnO_3$. A modified IR spectrum, with a very strong and broad band centered at 452 cm^{-1} and a marked shoulder at 580 cm^{-1}, is generated by a superposition of the NiO and $NiMnO_3$ spectra.

References

1. N. Valverde Diez, *J. Amer. Ceram. Soc.* **68,** 657 (1985).
2. N. Valverde Diez and D. Grande Fernandez, *Solid State Ionics* **28–30,** 1697 (1988).
3. Yu V. Golikov and V. F. Balakirev, *J. Phys. Chem. Solids* **49,** 329 (1988).
4. D. G. Wickham, *J. Inorg. Nucl. Chem.* **26,** 1369 (1964).
5. P. Porta and M. Valigi, *J. Solid State Chem.* **6,** 344 (1973).
6. J. S. Kasper and J. S. Prener, *Acta Crystallogr.* **7,** 246 (1954).
7. E. Dubler, A. Vedani, and H. R. Oswald, *Acta Crystallogr. Sect. C* **39,** 1143 (1983).
8. J. J. Fahey, *Amer. Mineral.* **40,** 905 (1955).
9. U. Takahashi and Y. Sakamoto, *J. Sci. Hiroshima Univ. Ser. A Phys. Chem.* **24,** 647 (1960).
10. H. S. Horowitz and J. M. Longo, *Mater. Res. Bull.* **13,** 1359 (1978).
11. J. M. Longo, H. S. Horowitz, and L. R. Clavenna, "Solid State Chem.: A Contemporary Overview," (S. L. Holt, J. B. Milstein, and M. Robbins, Eds.) Adv. Chem. Series 186 Amer. Chem. Soc., Washington DC (1980).
12. X-Ray Powder Data File, ASTM 11-31.
13. R. D. Shannon, *Acta Crystallogr. Sect. A* **32,** 751 (1976).
14. A. Cimino, M. Lo Jacono, P. Porta, and M. Valigi, *Z. Physik. Chem. N. F.* **55,** 14 (1967).
15. R. Pappalardo, D. L. Wood, and R. C. Linares, *J. Chem. Phys.* **35,** 4041 (1961).
16. G. R. Rossman, R. D. Shannon, and R. K. Waring, *J. Solid State Chem.* **39,** 277 (1981).
17. P. Porta, F. S. Stone, and R. G. Turner, *J. Solid State Chem.* **11,** 135 (1974).
18. D. M. Adams and D. C. Newton, *J. Chem. Soc. A,* 2822 (1970).
19. D. M. Adams, *Coord. Chem. Rev.* **10,** 183 (1973).
20. I. L. Botto and E. J. Baran, *Z. Anorg. Allg. Chem.* **480,** 220 (1981).
21. I. L. Botto and E. J. Baran, *Z. Anorg. Allg. Chem.* **444,** 282 (1978).
22. M. T. McDevitt and W. L. Baun, *Spectrochim. Acta* **20,** 799 (1964).
23. N. Ogita, M. Udagawa, K. Kojima, and K. Ohbayashi, *J. Phys. Soc. Japan* **57,** 3932 (1988).